**48th AIAA/ASME/ASCE/AHS/ASC Structures, Structural Dynamics, and Materials Conference
23 - 26 April 2007, Honolulu, Hawaii**

AIAA 2007-1820

A Test Method to Assess the Foldability of Flexible Structural Materials

Thomas W. Murphey[*]

Air Force Research Laboratory, Kirtland AFB, NM 87117

and

Gregory E. Sanford[†]

CSA Engineering, Inc., Albuquerque, NM 87123

A coupon level comparative test method was developed to assess the foldability of thin flexible materials used in deployable structures. The subject materials support tensile and compressive loads; they are not cloth-like. The non-destructive method consists of a tensile stiffness test and a compressive buckling test and reveals changes in coupon properties that could result from locally extreme strains incurred during folding. The test is intended to provide a standardized means to compare changes in material systems or fabrication processes as flexible material development efforts continue. The method was applied to nine identical rigidizable composite coupons folded ten times. Five of the coupons were folded to a 4 mm radius and four were folded to a 2 mm radius. The results did not reveal a measurable change in coupon behavior from the pre-folded state.

Nomenclature

Symbols
D	=	plate bending stiffness
E	=	Young's modulus
L	=	coupon free length
P	=	buckling load
t	=	coupon thickness
w	=	coupon width
υ	=	Poisson's ratio

I. Introduction

Material deformation based deployable structures employ tensile and compressive material strains to allow packaging and deployment of a structure. Heritage material deformation architectures have relied on recoverable elastic strains in materials that do not undergo chemical, phase or state transitions. Successful examples of these are continuous longeron masts[1] (CLM), which are typically made from S2 Fiberglass, and storable tubular extendible masts[2] (STEM), which are made from beryllium-copper or stainless steel. While these architectures compact to less than 1% of their deployed length, material deformation architectures with increased mass efficiency (structural hierarchy) and high compaction ratios have not been demonstrated.

The graphite fiber reinforced plastic (GFRP) DECSMAR architecture achieves a structural performance greater than a truss of solid rods, but high compaction ratios have not been achieved[3,4]. The similarly GFRP based ATK-COI developed TriLok® architecture simultaneously achieves high compaction ratios and performance similar to a truss of tubes, however, it can be argued that the architecture is not purely material deformation based because it is not monolithic. During deployment, three elastically stowed plate-like strips are assembled to form a triangular

---

[*] Research Engineer, Space Vehicles Directorate, 3550 Aberdeen Ave., Senior Member AIAA.
[†] Project Engineer, CSA Engineering, Inc., 1451 Innovation Pkwy. SE Suite 100, Member AIAA.

Report Documentation Page		*Form Approved* *OMB No. 0704-0188*

Public reporting burden for the collection of information is estimated to average 1 hour per response, including the time for reviewing instructions, searching existing data sources, gathering and maintaining the data needed, and completing and reviewing the collection of information. Send comments regarding this burden estimate or any other aspect of this collection of information, including suggestions for reducing this burden, to Washington Headquarters Services, Directorate for Information Operations and Reports, 1215 Jefferson Davis Highway, Suite 1204, Arlington VA 22202-4302. Respondents should be aware that notwithstanding any other provision of law, no person shall be subject to a penalty for failing to comply with a collection of information if it does not display a currently valid OMB control number.

1. REPORT DATE **APR 2007**	2. REPORT TYPE	3. DATES COVERED **00-00-2007 to 00-00-2007**
4. TITLE AND SUBTITLE **A Test Method to Assess the Foldability of Flexible Structural Materials**		5a. CONTRACT NUMBER
		5b. GRANT NUMBER
		5c. PROGRAM ELEMENT NUMBER
6. AUTHOR(S)		5d. PROJECT NUMBER
		5e. TASK NUMBER
		5f. WORK UNIT NUMBER
7. PERFORMING ORGANIZATION NAME(S) AND ADDRESS(ES) **CSA Engineering Inc,1451 Innovation Parkway SE,Albuquerque,NM,87123**		8. PERFORMING ORGANIZATION REPORT NUMBER
9. SPONSORING/MONITORING AGENCY NAME(S) AND ADDRESS(ES)		10. SPONSOR/MONITOR'S ACRONYM(S)
		11. SPONSOR/MONITOR'S REPORT NUMBER(S)

12. DISTRIBUTION/AVAILABILITY STATEMENT **Approved for public release; distribution unlimited**

13. SUPPLEMENTARY NOTES **The original document contains color images.**

14. ABSTRACT

15. SUBJECT TERMS

16. SECURITY CLASSIFICATION OF:			17. LIMITATION OF ABSTRACT	18. NUMBER OF PAGES **13**	19a. NAME OF RESPONSIBLE PERSON
a. REPORT **unclassified**	b. ABSTRACT **unclassified**	c. THIS PAGE **unclassified**			

Standard Form 298 (Rev. 8-98)
Prescribed by ANSI Std Z39-18

truss.[5] Efficient architectures capable of high compaction ratios exist[6,7], the limitation is caused by a lack of materials that are both stiff and high strain.

It is an enduring challenge of the Deployable Structures Community to find or develop high strain materials. Fortunately, the unique requirements of deployable structures render this materials problem tractable. Materials for deployable structures only need to be stiff in the fully deployed configuration; the materials do not need to be stiff during deployment. In addition, the materials only need to accommodate high compressive strains; they do not need to both stretch and compress to high strain levels. Exploiting these requirements, rigidizable materials were developed to enable increased structural performance systems with high compaction ratios.[8]

Rigidizable materials are continuous GFRP laminates where the plastic (matrix) can be softened. In this softened state, the laminate can be folded because the fibers are allowed to microbuckle and otherwise move to accommodate effective strains much greater than traditional fiber and matrix systems can withstand.[9] Rigidizable materials are often formulated so that the matrix can be subsequently stiffened (rigidized), locking in the large effective strains. In a typically repeatable process, the matrix can later be softened, the large strains are recovered and the matrix is again rigidized in a deployed configuration. Several examples of structures built from rigidizable materials are described in Reference 5.

Material deformation based deployable structure designers, whether using rigidizable or elastic GFRP, often arrive at an architecture that employs thin composite laminates in tube or tape-spring like cross sections. Thinner laminates reduce the strain required for bending structures to a small radius (i.e. folding). Once deployed, the laminate is required to have in-plane stiffness to provide global structural stiffness. In addition, the laminate must have bending stiffness to resist buckling (the need for laminate bending stiffness to resist buckling is exacerbated by laminate thinness). Bulk material tensile or compressive strength is rarely a driving requirement. These laminate properties, in-plane (tensile and compressive) and bending stiffness, are the primary properties needed to design and predict deployed structural component performance. The proposed test method does not claim to measure these properties. Instead, the method measures laminate characteristics that are indicators of the above properties. The test method allows a flexible structural material to be tested, then folded and unfolded, and tested again. By comparing the pre-fold test results to the post-fold test results, an indication of change in the material is achieved.

The intent of the test is to provide an early assessment of new flexible structural materials. The test is appropriate for screening changes in fiber, matrix or processing. It is also appropriate for comparing different classes of material systems. Structural component level testing is often more desirable than coupon level testing. However, it may be too expensive or otherwise impractical to perform repeated structural component testing. Further, the effects of material folding may be diluted at the structure level, effectively concealing local fold material performance information from consideration.

In the following section, the challenges of foldability assessment will be described along with finite element analysis simulations that support the proposed test approach. The proposed test protocol is presented in Section III and lastly, the test protocol will be applied to a contemporary rigidizable material system in Section IV.

II.   Foldability Assessment

The proposed test method includes a tensile test to measure the tensile modulus of the coupon and an elastic buckling test to measure the material's ability to carry load. Both tests are conducted on the same 2.5 x 25 cm tabbed coupon. An example is shown in Figure 1. These tests were selected: 1) because they assess the coupon level characteristics that most strongly and directly influence a thin laminate's performance in a structural component and 2) because they are readily implemented without the need for extensive specialized tooling. Several additional constraints influenced selection of these tests. The test method needs to be non-destructive so that the same coupon can be tested, folded and tested again. This avoids the requirement that an unreasonably large number of coupons should be tested to achieve statistical confidence between different coupons. Also, folding precludes testing of very small coupons because they must be large enough to fold. The influence of folding can extend well beyond the actual fold region.

The two tests necessitate some assumptions. It is assumed that laminate folding damage will manifest as a change in tensile stiffness of the laminate. If a large number of fibers break during folding, it is reasonable that this test would reveal a reduction in modulus. Similarly, delamination or other matrix failures could result in the fibers retaining waviness after folding. This would also reasonably manifest as a reduction in tensile modulus as the fibers are pulled from a wavy to a straighter condition. A compressive modulus test would also be a good indicator of laminate performance since a compressive load would tend to increase any pre-existing delaminations or fiber waviness. A compression test that meets the non-destructive objectives of this study could not be found.

A buckling test was selected for the second test only after careful consideration. Two boundary conditions were examined through finite element analysis simulations of a 38 mm long x 25 mm wide x 0.3 mm thick aluminum coupon with a central 10 mm long reduced elastic modulus fold region. Pinned-pinned boundary conditions were considered first because they concentrate the bending deformations towards the center of the coupon. However, pinned-pinned boundary conditions require a short coupon and complicate folding. Fixed-fixed boundary conditions were not expected to be as sensitive to a modulus reduction because deformations occur at the coupon ends as well as the center. Nonlinear load-displacement curves for each case are shown in Figure 2. As expected, the pinned-pinned case is more sensitive to a center region modulus reduction, though not dramatically. A 10% modulus reduction results in a 5.3% buckling load reduction in the pinned-pinned case and a 4.4% reduction in the fixed-fixed case. A 50% modulus reduction results in a 34% buckling load reduction in the pinned-pinned case and a 25% reduction in the fixed-fixed case. Due to their ease of implementation and relatively good sensitivity to a reduced modulus, fixed-fixed end conditions were selected.

The test fixture shown in Figure 3 was fabricated to clamp the coupon with fixed-fixed end conditions and a 38 mm long free section. Recessed tab cutouts are included to accommodate the full 25 cm length of the coupon within the clamps. The buckling test must be elastic so that laminate damage does not occur. To ensure this, coupon free length should be 100-200 times longer than it is thick. This slenderness guarantees the sample will buckle at a low stress, far from the bulk material compressive failure stress. Figure 4 shows the fixture mounted in the test machine with a buckled sample.

For sizing displacement and load sensors, the buckling load of a coupon can be estimated using the Euler column buckling equation, modified for an isotropic plate with fixed-fixed boundary conditions,

$$P_{cr} = \frac{4\pi^2 wD}{L^2}$$

where,

$$D = \frac{Et^3}{12\left(1 - \upsilon^2\right)}$$

Buckling tests are inherently sensitive to coupon mounting and test fixture misalignment. A series of finite element simulations were carried out to assess these sensitivities. The test is most sensitive to tab rotation in the plane of the coupon. Figure 5 shows that a tab rotation error of up to 0.1 deg does not significantly alter the final buckling load. This degree of mounting error is visible as a noticeable asymmetric out of plane deformation in the sample. Figure 6 shows out of plane deformations for 0.01, 0.05 and 0.5 deg mounting errors (deformations are shown to scale relative to the sample). In the 0.01 deg case, the 0.002 mm deformations are not clearly visible. However, at 0.05 deg, where test results just start to be impacted, the 0.4 mm deformations are greater than the material thickness and are visible.

Tab twist and offset errors were also investigated. Figure 7 shows that a 2 mm tab offset (out of plane to the coupon) does not alter the final buckling load. Similarly, a 0.1 degree twist does not influence the test. The relative insensitivity of the buckling load to mounting errors is attributable to the buckled mode shape being a developable surface. A developable surface is a shape that can be formed from a flat sheet through purely inextensional bending deformations (i.e. it is not doubly curved). Developable surfaces are composed of cylindrical, conical and flat regions. Even large tab mounting errors do not prevent the coupon from buckling into a similar developable surface as when the coupon is perfectly mounted. This consistency in mode shape results in a similar consistency in buckling load.

Even so, buckling test results must be interpreted with caution. Two qualities of these buckling tests are meaningful. First, the final plateau buckling load provides a measure of the lengthwise integrated flexural stiffness of the coupon. Figure 2 shows the sensitivity of the buckling load to the flexural modulus of the fold region. Second, the sharpness of the knee in transitioning to a buckled state provides an indication of the initial straightness of the coupon. Coupon flatness imperfections (due to folding) have the effect of rounding what would otherwise be a crisp transition to the buckled state. This rounding is qualitative since it is difficult to numerically characterize the curve. In practice, it is difficult to distinguish mounting errors from coupon flatness errors and coupons that show significant transition rounding should be inspected for visual signs of initial flatness errors or mounting errors.

Figure 2 indicates that a reduction in modulus due to folding will be apparent in the initial slope of buckling test data. This data should be ignored. The initial slope of the buckling curve is sensitive to mounting errors as shown in Figure 5 and Figure 7. Additionally, displacement measurements are not accurate in this region because they are based on cross-head displacement, not coupon measurements.

III. Test Protocol

The following operations should be performed on the number of samples required for the desired statistical accuracy:

1. Prepare Coupons: Standard methods should be employed to mount 5 cm long pull tabs on coupons that are 2.5 cm wide x 25 cm long. The coupon width is chosen to ensure a plate-like behavior in the coupon, avoiding edge effects during buckling. Fabricating the coupons and trimming them such that their sides are precisely parallel simplifies precision mounting of the coupons for the buckling tests.
2. Tensile Stiffness Test: It is critical that the coupon be gripped without alignment errors. Even slight misalignments will result in a non-uniform load distribution across the sample and subsequent nonlinear behavior and premature coupon failure. In this study, the coupons were trimmed with precision parallel sides using a surface grinder. Precision gripping was ensured by butting these sides against the back of the grip heads, which were previously aligned. Due to the thinness of the laminates, an ideal instrument to measure coupon stretch is a laser extensometer. Strain gages should not be used because the average modulus over the region to be folded is desired. Further, strain gages would adversely influence the folding process. A mechanical extensometer was employed in this study because the tests were conducted in a low temperature environmental chamber that did not have an optical grade window. The weight of the mechanical extensometer presented mounting challenges and an 89 N preload was required before the extensometer could be mounted. For this study, the tensile modulus was calculated from a linear regression of the increasing load test data from 1,000 $\mu\varepsilon$ to 3,500 $\mu\varepsilon$.
3. Fixed-Fixed Buckling Test: Mount the coupon in the clamp fixture (Figure 3). In this study, the fixture employed guide pins to align the coupon with the clamp and, similar to the tensile test, the clamp was aligned with the back of the load head. A precision machined parallel with 2.5 cm width was used to set the coupon free length. With the lower grip still free, the machine load should be zeroed. At this point, the only weight on the coupon is the clamp and this should be subtracted from the test data. Activate the lower grip and visually inspect the coupon for planarity. It was found that movement could occur in the gripping process and cause a noticeable out of plane deformation in the coupon. When this happened, the lower grip was released and the process repeated until the coupon was free of visible deformations. The buckling test should be continued until a definite plateau load is apparent. In the study, coupons were compressed by 6,000 $\mu\varepsilon$. Plateau stresses are reported as the average stress from 3,000 to 4,000 $\mu\varepsilon$.
4. Fold and unfold coupon using a folding procedure appropriate for the material.
5. Repeat Tensile Test (2).
6. Repeat Buckling Test (3).

IV. Rigidizable Material System Test Protocol Results

The test protocol was carried out on a rigidizable GFRP material system developed and fabricated by L'Garde Inc. The laminate was fabricated from an unbalanced woven fabric with L'Garde L5.5 resin and a nominal fiber volume fraction of 40%. While thickness among the 9 coupons ranged from 0.254 mm to 0.356 mm, a constant thickness of 0.305 mm was assumed for all samples. This assumes that fiber content is constant regardless of thickness and that fiber behavior is dominant. The coupon long axis was aligned parallel to the fabric warp direction. Coupons 16-20 were folded to a 4 mm radius and coupons 22-25 were folded to a 2 mm radius.

Folding of the laminate involves a cycle of heating to soften the matrix → laminate folding at high temperature → laminate unfolding at high temperature → cooling to rigidize the matrix in the deployed configurations. An environmental chamber was used to maintain temperatures at 90 C for folding and unfolding and -40 C for tensile and buckling tests. Prior to tensile testing, the coupon was cooled for 10 min in a previously cooled chamber. Folding was accomplished using an automated folding fixture located within the environmental chamber and controlled through cross-head motion in the test machine. The folding apparatus uses a spring to tension the coupon and hold it against the folding mandrel (either 4 or 2 mm radius) as shown in Figure 8. The spring force is approximately 5 N when the coupon is straight and 10 N when the coupon is fully folded. The folding fixture was heated at 90 C for 30 min prior to loading a coupon. After loading a coupon, the assembly was heated at 90 C for an additional 10 min. Folding and unfolding were accomplished without opening the chamber. Samples were not cooled after folding and were not cooled between consecutive fold-unfold cycles. On the final unfold cycle, the coupons were given 5 min to fully straighten before cooling was initiated.

Results for all stiffness tests are summarized in Table 1 and all buckling tests in

Table 2. Test results are also plotted in Figure 9, Figure 10 and Figure 11. The results show a linear stiffness response before and after folding. Overall, there is a 4.2% decrease in modulus in going from the pristine condition to folded ten times. This slight decrease is within the standard deviation of the test data and does not constitute a measurable decrease in modulus. Close inspection of the stiffness data revealed that all but one (10.86 Msi) of the stiffness measurements over 10.68 Msi exhibit an apparent coupon shrinkage in the test data. This could be an artifact of the extensometer mounting, not real material behavior. The weight of the extensometer and the pressure from its mounting clips at times caused the sample to deform. The lowest stiffness curves exhibited unexplainable discrete changes in slope. Generally, coupons that had fewer artifacts in their stress-strain curves also showed less scatter in their modulus regression data. There is insufficient evidence to attribute the observed variations in modulus to laminate damage.

Each buckling test was performed twice, re-gripping the clamps between tests. The resulting plateau stresses were highly consistent, typically varying by less than 2%. This consistency indicates observed behaviors are not a result of coupon mounting errors. The plateau stresses among different samples and after folding showed much greater variation. However, a consistent increase, decrease or other trend in buckling load was not observed. The observed variation in buckling load is believed to be a true coupon behavior change resulting from the folding and unfolding process. It is possible that the spring used in the folding fixture to pull the coupons straight after unfolding did not always provide sufficient straightening force. This would result in a slight kink in the coupon and cause the buckling load-deflection curve to be highly rounded and plateau at a lower stress.

V.   Discussion and Conclusion

Folding deformations have the potential to cause delamination, fiber breakage and matrix cracking. This folding damage is not detrimental to the use of flexible structural materials in deployable structures. Predictable performance is the fundamental requirement to use the material in engineered systems and damage does not inherently preclude achieving predictable performance. If folding results in a measurable level of material performance that can be statistically characterized through repeated tests, then the system using it can be rationally engineered. Predicting this laminate folding damage analytically is likely an intractable approach. Alternatively, repeated statistically significant observations of material performance will provide the experience based confidence required for flight use of advanced materials.

A method was presented to assess the foldability of flexible structural materials and the test was performed on a rigidizable laminate repeatedly as the material was folded and unfolded ten times. The test method did not conclusively reveal degradation in material laminate performance with folding. This result provides good evidence the L'Garde material robustly handles repeated folding. However, it provides little insight into the quality of the test protocol itself. It may prove useful to continue the test protocol on the same L'Garde samples, using successively smaller folding mandrels until the test results clearly indicate a reduction in performance. With such information, the value of the test protocol could be assessed. For example, if coupons show unacceptable visible laminate damage that does not manifest in the test results, the test is of limited use. However, if the test results reveal degradation in performance and laminate damage is not clearly visible, then the test would provide useful information.

The authors acknowledge the limitations and challenges associated with the proposed test protocol. After exercising the method on a thermally demanding material system, it is believed the test method warrants continued use and improvements. A laser extensometer is expected to improve the stiffness measurements. A more robust folding and unfolding protocol is expected to reduce the variation in buckling test results.

References

[1]Mauch, H.R., "Deployable Lattice Column," US Patent 3486279, 1969.
[2]NASA Space Vehicle Design Criteria (Guidance and Control), "Tubular Spacecraft Booms (Extendible, Reel Stored)," NASA SP-8065, 1971.
[3]Pollard, E.L. and Murphey, T.W., "Development of Deployable Elastic Composite Shape Memory Alloy Reinforced (DECSMAR) Structures," *Proceedings of the 47th AIAA/ASME/ASCE/AHS/ASC Structures, Structural Dynamics, & Materials Conference*, AIAA-2006-1681.
[4]Pollard, E.L. et al., "Experimental and Numerical Identification of DECSMAR Structures' Deployment and Deployed Performance," *Proceedings of the 48th AIAA/ASME/ASCE/AHS/ASC Structures, Structural Dynamics, & Materials Conference*, AIAA-2007-2004.
[5]Murphey, Chapter 1: Booms and Trusses, Recent Advances in Gossamer Spacecraft, Ed. Jenkins, C., AIAA, 2006.

[6]Mejia-Ariza, J.M., Murphey, T.W. and Pollard, E.L., "Manufacture and Experimental Analysis of a Concentrated Strain Based Deployable Truss Structure," *Proceedings of the 47th AIAA/ASME/ASCE/AHS/ASC Structures, Structural Dynamics, & Materials Conference*, AIAA-2006-1686.

[7]Pollard, E.L. et al., "Experimental and Numerical Identification of MACSES Structures' Deployment and Deployed Performance," *Proceedings of the 48th AIAA/ASME/ASCE/AHS/ASC Structures, Structural Dynamics, & Materials Conference*, AIAA-2007-2007.

[8]Freeland, R. E., Bilyeu, G. D., Veal, G. R., and Mikulas, M. M., "Inflatable Deployable Space Structures Technology Summary," 49th Congress of the International Astronautical Federation, IAF-98-1.5.01, Sept. 1998.

[9]Murphey T.W. and Mikulas, M.M., "Some Micromechanics Considerations on the Folding of Rigidizable Composite Materials," *Proceedings of the 42nd AIAA/ASME/ASCE/AHS/ASC Structures, Structural Dynamics, & Materials Conference*, AIAA-2001-1418.

Table 1: Stiffness test results (coupons 16-20 folded at 4 mm radius, coupons 22-25 folded at 2 mm radius).

				Stiffness (E_1, Msi)					
Coupon #	ROM Prediction	0 Folds	1 Fold	3 Folds	4 Folds	5 Folds	7 Folds	8 Folds	10 Folds
16	11.87	10.44	10.25	10.49		10.44		9.61	10.11
17	11.87	10.71	10.83	10.45		10.12		10.25	9.99
18	11.87	10.86	10.08	10.68		10.61		10.47	10.67
19	11.87	10.79	11.63	10.34		9.32		10.90	9.55
20	11.87	11.01	10.36	10.27		11.39		10.33	10.39
22	11.87	9.62	10.51		9.95		9.69		10.01
23	11.87	10.45	9.77		9.65		9.96		10.14
24	11.87	10.20	10.13		10.02		10.38		10.18
25	11.87	10.68	10.35		11.25		10.03		9.72
Max.	11.87	11.01	11.63	10.68	11.25	11.39	10.38	10.90	10.67
Min.	11.87	9.62	9.77	10.27	9.65	9.32	9.69	9.61	9.55
Avg.	11.87	10.53	10.43	10.45	10.22	10.38	10.02	10.31	10.09
Std. Dev. (%)	0.0%	4.0%	5.1%	1.5%	6.9%	7.2%	2.8%	4.5%	3.3%

Table 2: Buckling load test results (coupons 16-20 folded at 4 mm radius, coupons 22-25 folded at 2 mm radius).

				Buckling Load (σ_{cr}, ksi)					
Coupon #	Predicted	0 Folds	1 Fold	3 Folds	4 Folds	5 Folds	7 Folds	8 Folds	10 Folds
16	2,318	961	935	1,030		970		965	990
17	2,318	1,038	945	905		818		909	1,033
18	2,318	1,060	954	1,094		1,038		1,096	1,138
19	2,318	939	821	935		933		808	1,019
20	2,318	880	857	922		914		894	1,069
22	2,318	1,064	1,108		924		1,038		985
23	2,318	958	901		957		945		870
24	2,318	1,087	1,084		1,103		1,041		1,020
25	2,318	1,096	1,053		1,061		1,031		1,042
Max.	2,318	1,096	1,108	1,094	1,103	1,038	1,041	1,096	1,138
Min.	2,318	880	821	905	924	818	945	808	870
Avg.	2,318	1,009	962	977	1,011	934	1,014	934	1,018
Std. Dev. (%)	0.0%	7.6%	10.4%	8.3%	8.4%	8.6%	4.5%	11.4%	7.1%
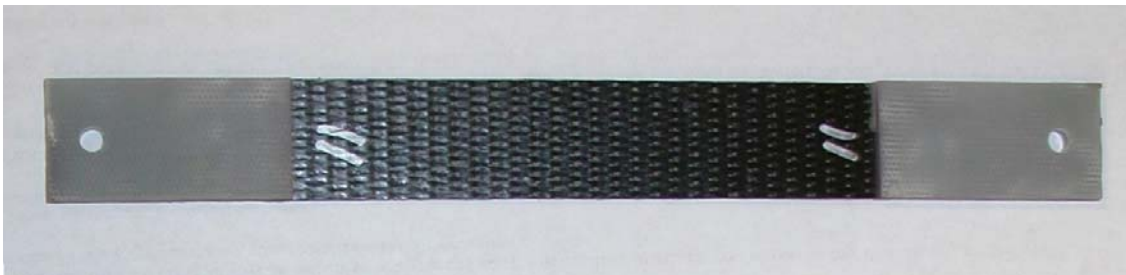
Figure 1: Rigidizable material test coupon.
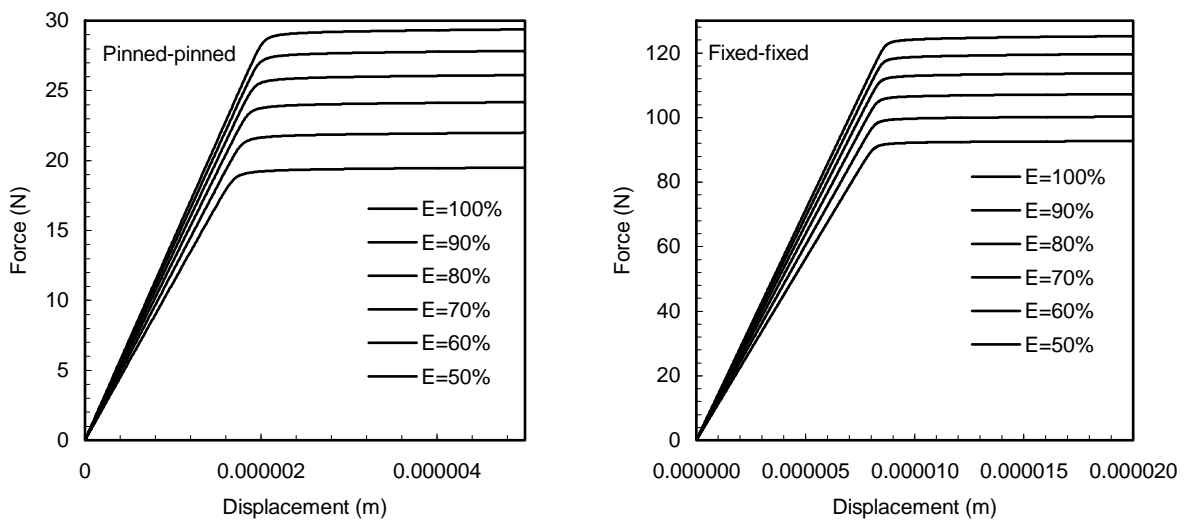
Figure 2: Finite element simulation of buckling test with pinned-pinned and fixed-fixed end conditions.

Figure 3: Buckling test fixed-fixed support clamps.

Figure 4: Buckling test setup showing buckled sample.
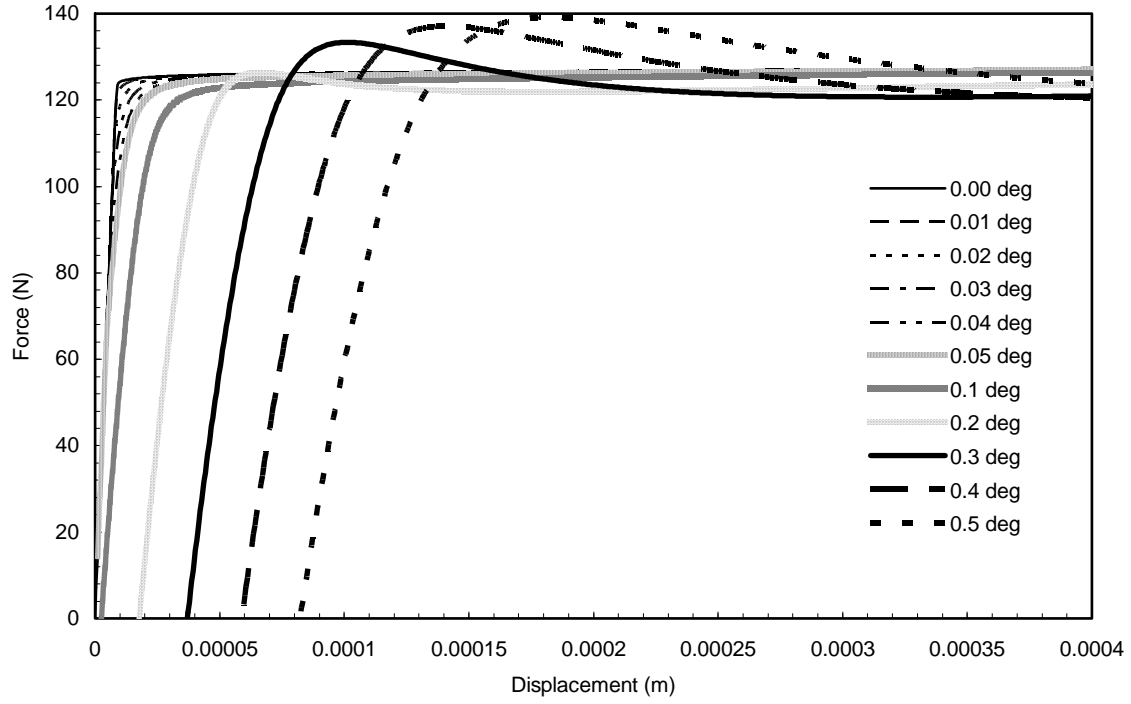
Figure 5: Finite element simulation of buckling test with upper tab rotational error.
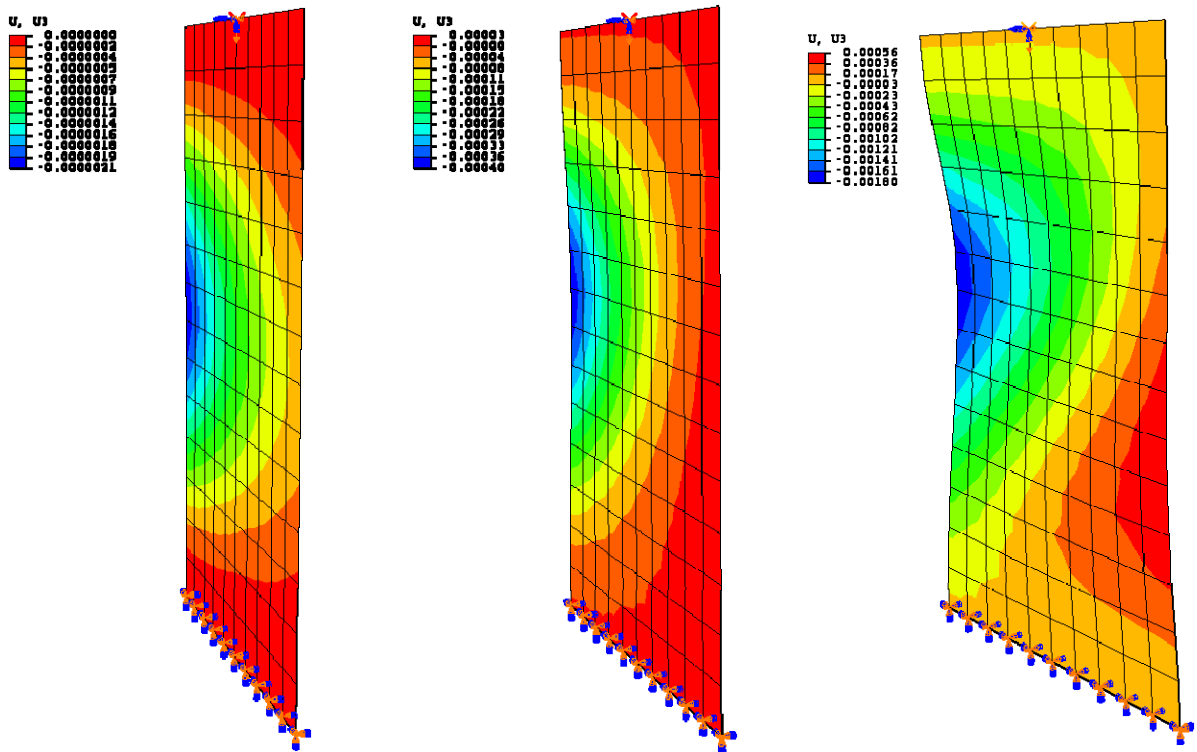
Figure 6: Transverse deformations in samples mounted with 0.01, 0.05 and 0.5 degrees of tab rotation in the upper grip (deformations to scale relative to coupon).

American Institute of Aeronautics and Astronautics
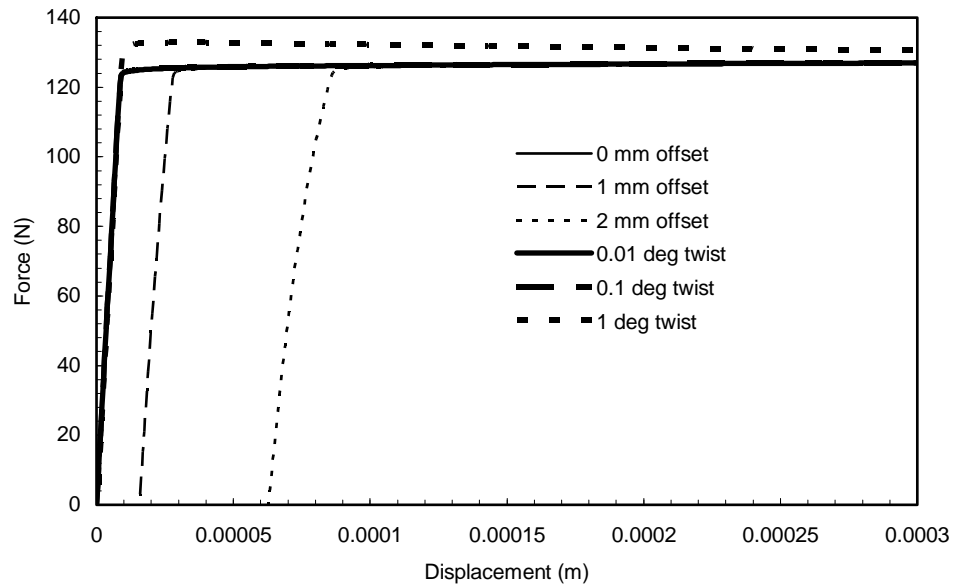
Figure 7: Finite element simulation of buckling test with upper tab grip offset and twist errors.

Figure 8: Folding apparatus within the environmental chamber and shown first unfold and second, folded.
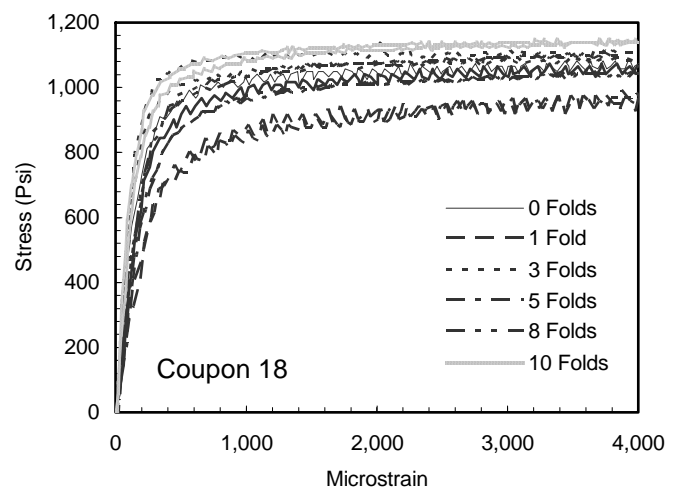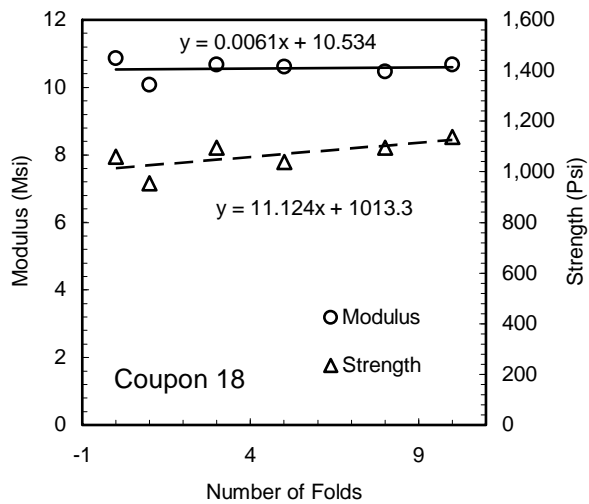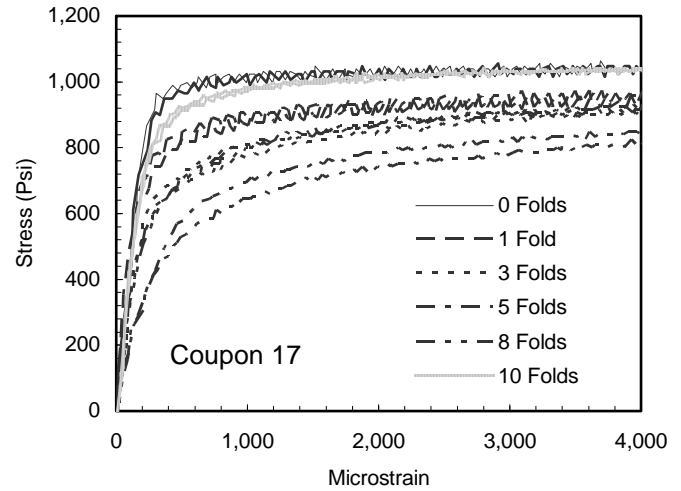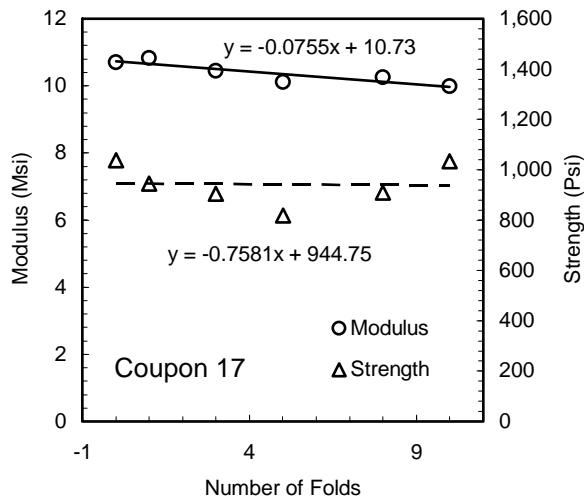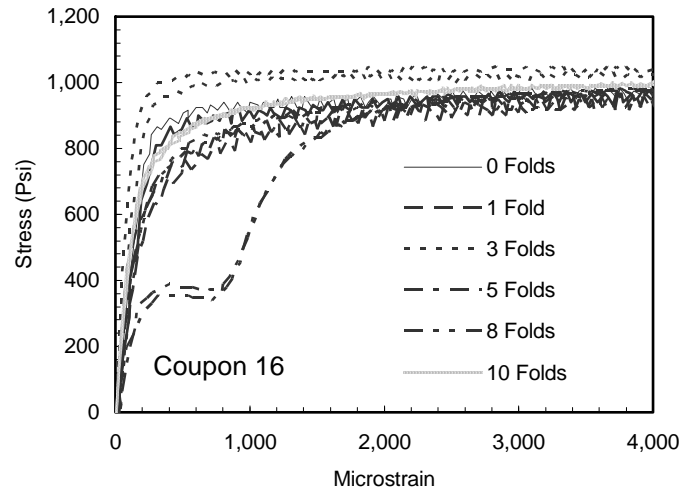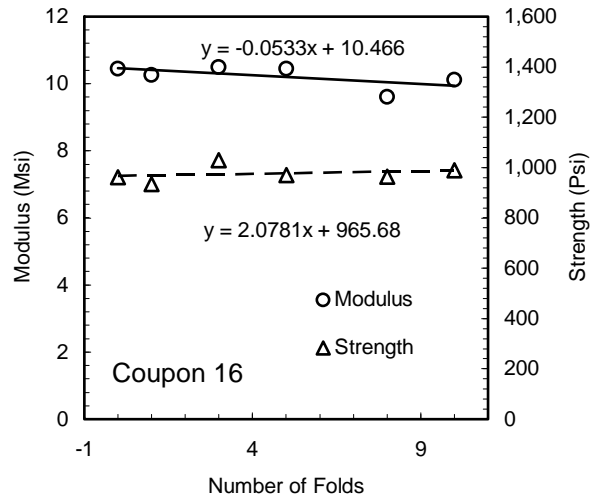
Figure 9: Coupons 16, 17 and 18 test results.
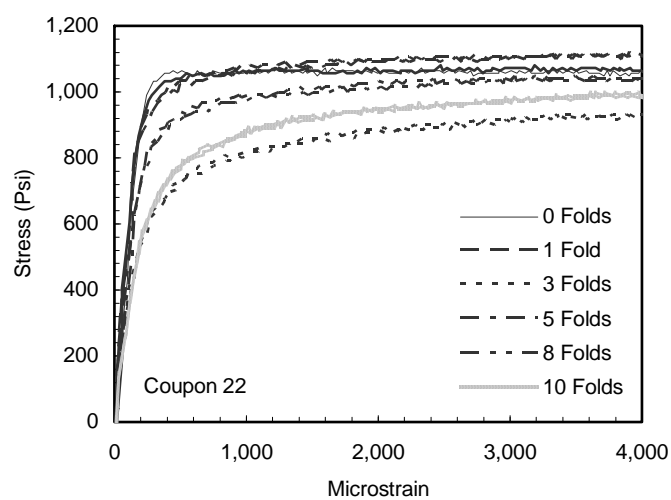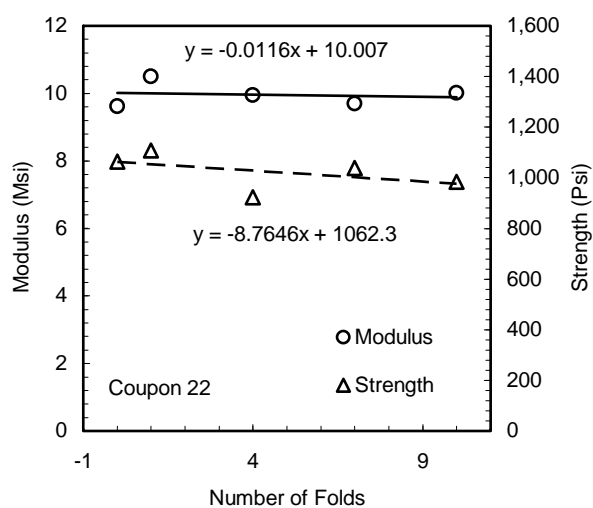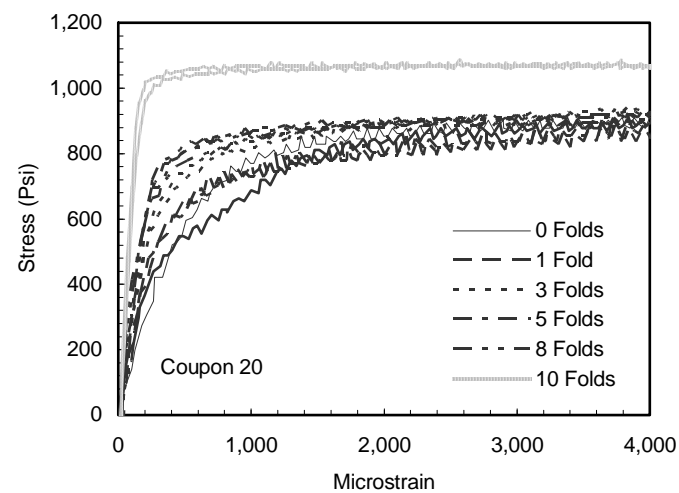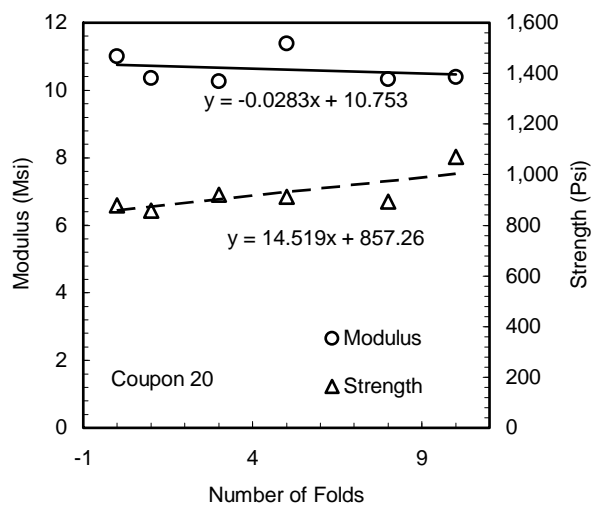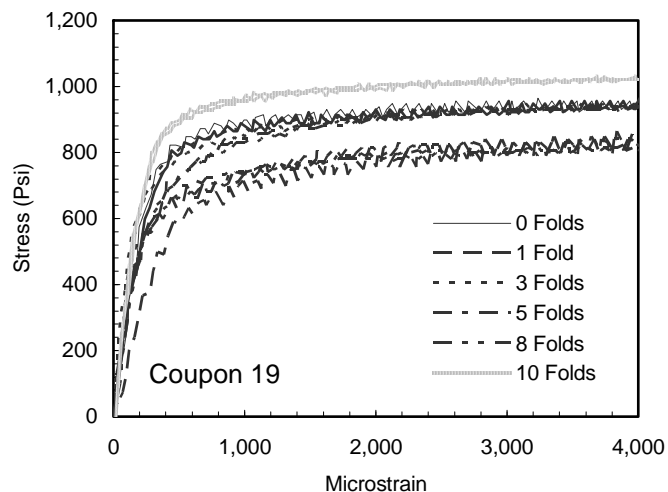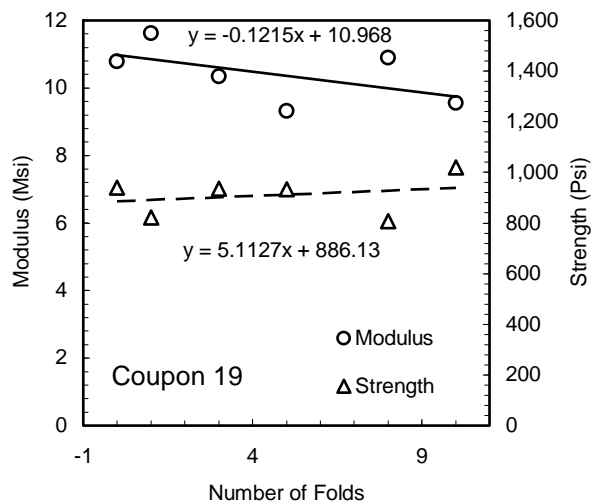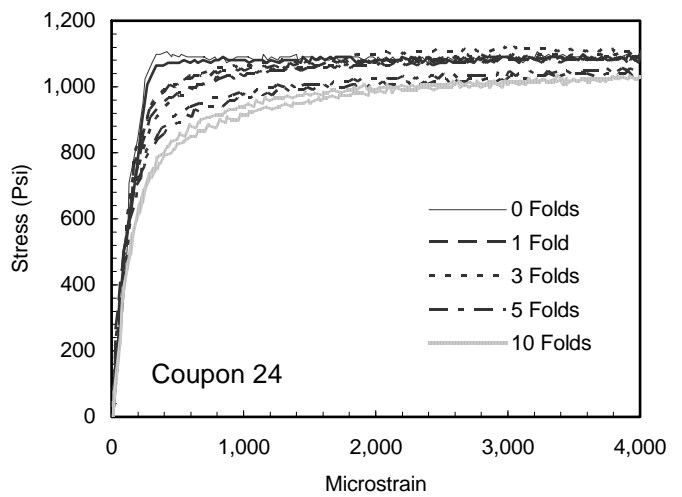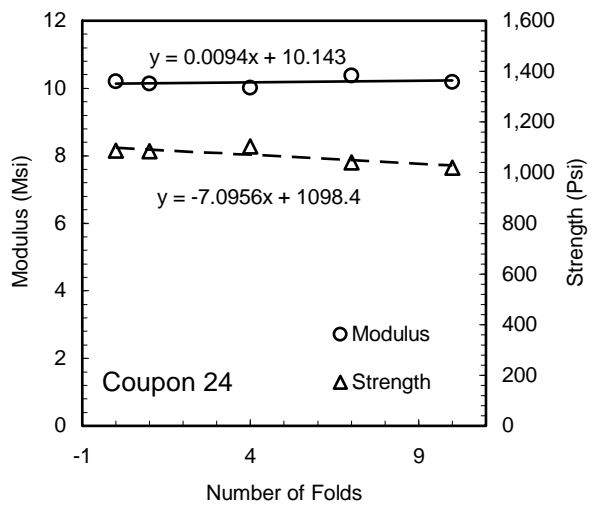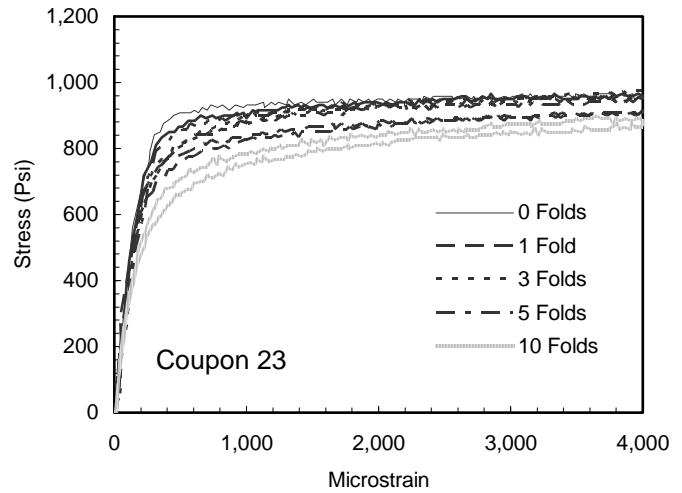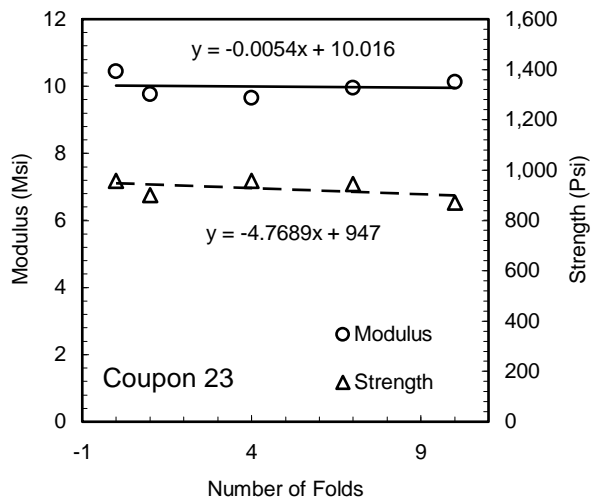
Figure 10: Coupons 19, 20 and 22 test results.
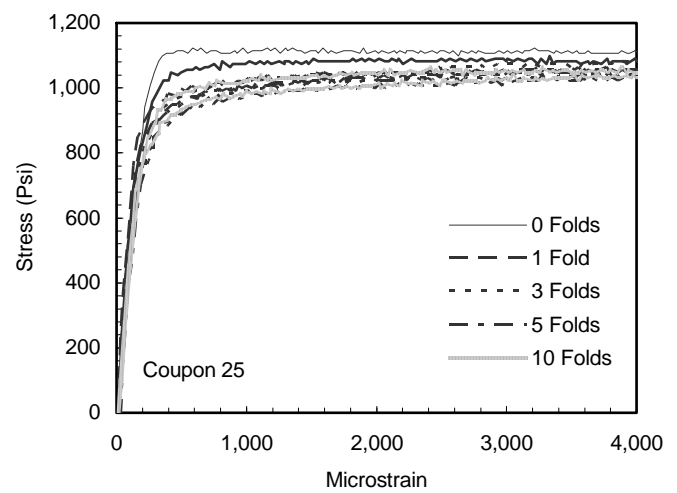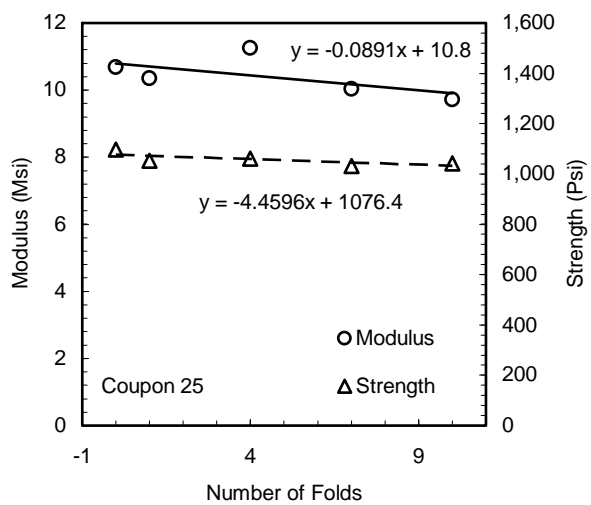
Figure 11: Coupons 23, 24 and 25 test results.